International Journal of GEOMATE, Nov., 2024 Vol.27, Issue 123, pp.1-10
ISSN: 2186-2982 (P), 2186-2990 (O), Japan, DOI: https://doi.org/10.21660/2024.123.4575
Geotechnique, Construction Materials and Environment

PERFORMANCE LEVEL IMPROVEMENT OF STEEL FRAME BUILDING EQUIPPED WITH OPTIMIZED ACTIVE TENDON SYSTEM

*Socio Jiwapatria[1], Herlien Dwiarti Setio[1], Indra Djati Sidi[1], and Patria Kusumaningrum[1]

[1]Department of Civil Engineering, Faculty of Civil and Environmental Engineering, Institut Teknologi Bandung, Indonesia

*Corresponding Author, Received: 29 May 2024, Revised: 06 Sep. 2024, Accepted: 08 Sep. 2024

ABSTRACT: The optimized active control system is tested on a steel-framed benchmark building to enhance the structure's performance level against seismic loads. The building is equipped with active tendon actuators at predetermined locations to counteract the external seismic forces. The optimal actuator configuration is searched using PMR-NSGA-II (Population Guided & Modified Reference-Point Based Non-Dominated Sorting Genetic Algorithm-II) to provide an effective and economical control system arrangement. The analysis is conducted via the 3D nonlinear time history analysis considering tri-directional excitations. The performance assessments at the structural and element levels are undertaken to evaluate the building's performance level per FEMA 356 and ASCE41-17, respectively. The active tendon system could effectively suppress the structure's dynamic response against various seismicity levels. The additional dissipation capacity provided by the control force could effectively reduce the yielding and damage of the structural elements. The inter-story drifts are reduced from a range of 2.07%-5.30% to 0.66%-1.92% in the X-direction and from a range of 0.4%-1.23% to 0.4%-0.89% in the Y-direction. The performance level of the structural elements is improved to be 100% below the IO level for all ground motions, except for the Chi-Chi record, where only 13.44% of elements are experiencing the IO-to-LS level. The control system offers great merits in protecting the building against seismic hazards, thus mitigating adverse effects on human activities and safety.

Keywords: Active tendon system, Nonlinear time history analysis, Performance level, Steel building, Vibration control

1. INTRODUCTION

The design principle of conventional seismic-resistant buildings depends on the dissipation mechanism in the form of yielding or damages at preferred locations. By allowing a structure to deform non-linearly, a designer accepts that part of the energy imparted into the structure will be dissipated inelastically and possibly lead to permanent deformations. The target performance of the conventional approach is preventing casualties and ensuring the building's stability and integrity after excitation so that collapse can be prevented.

For essential buildings, no or limited structural damage is expected to ensure immediate occupancy and continuation of human activity [1]. This requirement could mainly be realized by ensuring sufficient seismic capacity, which may lead to enormous construction costs for new buildings. Furthermore, a retrofit strategy shall be conducted for existing buildings to alleviate the seismic performance if deficiencies exist. A few reasons to retrofit existing buildings are more stringent new seismic codes [2], rising natural hazard levels, or aging and deteriorated buildings.

Structural damages may happen after a strong seismic event, and the building shall be assessed to determine whether it is deemed safe for future operation or needs retrofitting. Previous efforts have covered various solutions to enhance the building's seismic performance [3-5]. The seismic design principles are divided into a conventional approach and the usage of the vibration control system, which is also referred to as "smart structure" technology.

The conventional design approach involves using engineered construction material, developing lateral load-bearing elements, and selecting a structural system that could provide sufficient strength, ductility, and dissipation mechanisms. For example, an improvement of infill masonry wall connection was proposed to enhance the seismic performance of steel buildings [6]. An engineered material solution was proposed in the mid- and high-rise buildings using engineered cementitious composite (ECC), which could improve the building's seismic performance by using a lower-density material, hence reducing the dead load [7]. The use of other engineered materials, such as ferrocement and Carbon Fiber Reinforced Polymer (CFRP), to increase the strength of structural elements was also proposed with promising results [8-10].

The trends show increased control system application on civil structures as it has become more economically affordable [11-15]. The smart structure consists of a base isolator, passive, semi-active, active, and hybrid systems. The control

system offers significant merits, which can prevent structural damage and improve serviceability, resilience, and adaptivity towards natural hazards.

The efficacy of base isolators and passive dissipation devices to reduce building vibration has been demonstrated [16-20]. The principle of passive devices in reducing damages is to provide energy-dissipation capacity rather than increase the structural element strength capacity. Passive control using TMD was conducted to improve the performance level of the steel moment-resisting frame [21]. Hybrid systems combining two or more lateral load-bearing systems are also explored [22].

In general, the passive approach could alleviate the seismic performance of the buildings only for a few particular modes of vibration since the devices were designed to handle a few dominant modes only. The semi-active and active control system offers a superior feature to the passive counterpart, which could handle a wider excitation frequency bandwidth and provide a higher adaptivity against uncertain excitations.

Various passive devices provide the auxiliary energy dissipation capacity with multiple principles such as friction, heat transfer, and metallic yielding. As for semi-active and active control systems, actuators powered by external power sources counteract the excitation by providing a control force that may be introduced to change the control devices' characteristics or directly transfer the control force into the structure.

The active control system can alter the structure stiffness and damping behavior by introducing control forces proportional to the displacement and velocity responses. Previous studies have covered active control applications on building structures excited by bi-directional horizontal and vertical excitations [23]. The building is modeled using the MDOF system with a coupled torsional degree of freedom. The study could assess the structural response in terms of translational and rotational DOFs but cannot elaborate on the forces and stresses that are experienced by the elements.

A new paradigm is proposed to utilize dissipation devices that can improve the performance level of a building so that it ensures not only zero casualties but also the continuation of human activity, business continuity, and resilient societies [24]. The elevated performance levels shall reduce or diminish the repair and demolition cost of a damaged building after a strong seismic event. The proposed approach is attractive from the investment point of view. The initial cost of control system procurement shall outweigh the tangible and intangible costs related to casualties, building repair, and loss of revenue caused by disruption in operation. Less disturbance in society activities also means greater economic sustainability at the regional or national level.

This study is motivated to assess the performance level improvement of buildings equipped with an optimized active control system. The active control system was chosen due to its flexibility of design and tuning, which is also highly adaptive against excitations with a wide frequency bandwidth.

The performance-based design (PBD) approach is applied to streamline the economic design of the active control system to meet predefined performance criteria set by the designer. PBD prioritizes flexibility, enabling engineers to adjust designs according to the structure's importance, location, and budgetary constraints [25-26]. The performance-based design (PBD) has become more widely accepted due to its superiority over the strength-based method [27] where the structure's performance is evaluated based on the damage state.

2. MODEL DESCRIPTION

2.1 Building Model

The study analyzes a 20-story steel-framed benchmark building using the 3D nonlinear time history analysis. The structure was prepared as a benchmark model for nonlinear seismic analysis [28]. The preliminary checks show that there is SCWB non-conformance in the X-direction of the building due to the weak axis of the steel columns, which are all uniformly aligned. The material properties conform to ASTM A36 for the beams, ASTM A992 for the columns, and ASTM A500 for the box section columns. The building typology is seismic moment frame in both directions. The building has two stories of basement and has hinge supports at the base of all columns. At the ground level, the perimeter nodes are all X- and Y-translationally restrained to model the fixation level due to soil confinement around the building.

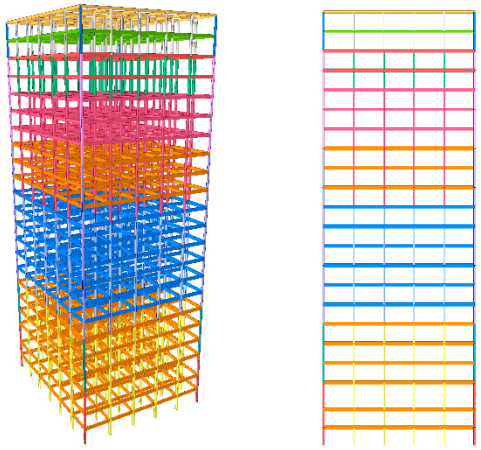

Fig.1 Isometric model of the benchmark steel-framed building a) 3D view b) Section view

The building is 5 bays × 6 bays in the X- and Y-directions, respectively, and has a 30.5 × 36.6 m^2 building area. The total height of the building is 88.03 m, measured from the B2 to the 20th story. All of the beam-column joints are assumed to be rigidly connected. The section properties of the structural element are presented in Table 1. The floor diaphragm considers the in-plane action of the concrete floor deck with a thickness of 15 cm. The concrete floor deck is simply supported by steel beam elements without using shear connectors.

Table 1. Section properties

Member Type	Section	Story
Column	W24×335	B2-3
	W24×229	4-10
	W24×192	11-13
	W24×131	14-16
	W24×117	17-18
	W24×84	19-20
	B15×15×5.08	B2-1
	B15×15×3.18	2-4
	B15×15×2.54	5-13
	B15×15×1.91	14-18
	B15×15×1.27	19-20
Beam	W30×99	B1, GF, 1-4, 11-13
	W30×108	5-10
	W24×131	14-16
	W27×84	17-18
	W24×62	19
	W21×50	20

2.2 Material Model

The material non-linearity considers infinitesimal 1D elasto-plasticity. The plasticity uses the combined isotropic-kinematic hardening governed by the Bauschinger effect parameter, β, for 0≤β≤1. For pure isotropic hardening, the value of β is 1; for pure kinematic hardening, the value of β is 0. The value of the Bauschinger effect parameter, β, is set to be 0.4. The convergence norm utilizes the residual force norm with a convergence tolerance of 0.001.

Table 2. Steel Material properties

Parameter	Value
Young's modulus, E	200000 MPa
Poisson's ratio, v	0.3
Yield strength, f_y	250 MPa for beams 345 MPa for columns
Material model	One-dimensional elastoplastic combined isotropic & kinematic hardening
Plastic modulus, H	2020.2 MPa
Bauschinger effect, β	0.4

2.3 Ground Motion Records

The ground motions consist of 5 records with various values of magnitude, PGA, and significant duration to demonstrate the efficacy of the control system against various seismic levels and to ensure record-to-record variation of the ground motions.

Table 3. Ground motion records

Ground Motion	Magnitude (M_w)	PGA (g)	Significant Duration (s)
Imperial Valley-1940	6.95	0.281	24.20
Kobe-1995	6.9	0.312	7.00
Landers-1992	7.28	0.417	10.6
Chi-Chi-1999	7.62	0.760	8.70
Kocaeli-1999	7.51	0.208	37.2

2.4 Performance Level Acceptance Criteria

The performance level of the building at the structural level is assessed using FEMA 356 [29] Table C1-3 Structural Performance Levels and Damage. The acceptance criteria are based on the interstory drift value. The interstory drift limit is 0.7% for the Immediate Occupancy (IO) level, 2.5% for the Life Safety (LS) level, and 5% for the Collapse Prevention (CP) level.

The performance level at the structural level is conducted based on ASCE41-17 [30] Table 9-7.1 Modeling Parameters and Acceptance Criteria for Nonlinear Procedures – Structural Steel Beams and Columns – Flexural Action. The acceptance criteria are based on the plastic rotation angle of the column and beam elements.

3. CONTROL STRATEGY

3.1 Control System Design

The controlled equation of motion is expressed in Eq. (1), where the control force, $\{u(t)\}$, is introduced at the right-hand side of the problem. The matrix $[D]$ is the control force location matrix that dictates where the control force will be introduced to the structures.

$$[M]\{\ddot{x}(t)\} + [C]\{\dot{x}(t)\} + [K]\{x(t)\} = -[M]\{r\}\ddot{x}_g(t) + [D]\{u(t)\} \quad (1)$$

The second-order equation of motion is translated into the first-order equation of motion using the state space representation. The dynamic characteristic of the system is represented in the plant matrix $[A]$. The $[B_u]$ and $\{B_r\}$ are the input matrix and vector for the control force and the earthquake excitation, respectively. The n denotes the size of the degree of freedom of the system.

$$[A] = \left[\frac{[0]}{-[M]^{-1}[K]} \middle| \frac{[I]}{-[M]^{-1}[C]}\right]_{2n\times 2n} \quad (2)$$

$$[B_u] = \left[\frac{[0]}{[M]^{-1}[D]}\right]_{2n\times r} \quad (3)$$

$$\{B_r\} = \left[\frac{\{0\}}{\{[M]^{-1}[M]\{r\}\}}\right]_{2n\times 1} \quad (4)$$

The control force $\{u(t)\}$ is calculated based on the state variable vector $\{Z(t)\}$, which contains the displacement and velocity states of the system. The gain matrix $[G]$ is calculated using ROCA (Ricatti Optimal Control Algorithm) upon full-state-feedback assumption.

$$\{u(t)\} = -[G]\{Z(t)\} \quad (5)$$

The first-order equation of motion is expressed in Eq. (6). The gain matrix [G] is time-invariant and is obtained by solving the Ricatti equation.

$$\{\dot{Z}(t)\} = ([A] - [B_u][G])\{Z(t)\} + \{B_r\}\ddot{x}_g(t) \quad (6)$$

The search process to obtain the near-optimal configuration was conducted using metaheuristic optimization using PMR-NSGA-II [5], which utilized population guidance, a modified reference point, and non-dominated sorting. The PMR-NSGA-II could produce the optimal actuator configuration significantly quicker than the original NSGA-II [31].

Table 4. Number of actuators

Ground Motion	Imperial Valley		Landers		Kobe		Chi-Chi		Kocaeli	
Story	X	Y	X	Y	X	Y	X	Y	X	Y
1	2	2	2	2	2	2	4	4	2	0
2	2	2	2	0	0	0	4	0	2	0
3	2	2	2	2	0	2	4	4	2	0
4	0	0	2	0	0	0	0	0	0	0
5	2	0	2	0	2	2	4	0	2	0
6	2	0	0	0	0	0	4	0	2	0
7	0	0	2	2	0	2	0	4	0	0
8	2	0	0	2	2	0	0	4	2	0
9	2	0	2	2	0	2	0	4	0	0
10	0	0	0	2	2	0	4	4	0	0
11	0	0	2	0	0	0	4	0	0	0
12	2	0	0	0	0	2	0	0	2	0
13	0	0	0	0	0	0	4	0	0	0
14	2	0	0	0	0	0	4	0	0	0
15	0	2	0	0	2	0	4	0	0	0
16	2	0	0	0	0	0	4	0	2	0
17	0	0	0	0	2	0	4	0	0	0
18	2	0	2	0	0	0	4	0	2	0
19	2	0	0	0	0	0	4	0	0	0
20	0	0	0	0	0	0	2	0	0	0
Total	24	8	18	12	12	12	58	24	18	0

The control strategy aims to reduce the interstory drift of the buildings to satisfy the Immediate Occupancy level, where the interstory drift is targeted to be below 0.7%. The optimal placement and tuning of actuator devices are essential to safely ensure the appropriate level control force to counteract the external excitation upon performance level target.

Actuators are prepared in pairs per story and are placed in the outermost moment frames. Exceptionally, the Chi-Chi ground motion requires two pairs of actuators on most of the floors. The behavior of the building is more flexible and weaker in the X-direction than in the Y-direction due to the major axis of the column being oriented in the Y-direction. Hence, the optimal configuration in the X-direction requires more actuator devices than the Y-direction. Mostly, the first floor requires actuators to be placed for most of the ground motion records. The higher floor-to-floor elevation of the ground floor contributes to high lateral flexibility and soft story behavior of the 1st story.

3.2 Control Force Algorithm

The control algorithm utilizes ROCA (Ricatti Optimal Control Algorithm) with iterated weighing factors, γ, to adjust the control force in achieving the targeted control performance. The simple iterative process proposed [5] was proven dependable and computationally efficient in providing an optimized value of γ. The optimized gamma value for each ground motion is represented in Table 5.

Table 5. Weighting parameters for various ground motions

Ground Motion	γ	
	X-Dir [-]	Y-Dir [-]
Imperial Valley	1.73E-15	2.28E-14
Kobe	1.43E-14	3.33E-15
Landers	1.00E-14	1.63E-14
Chi-Chi	6.25E-16	2.50E-15
Kocaeli	1.00E-14	-

4. SIMULATION RESULTS & DISCUSSION

4.1 Performance Level at the Structural Level

The performance level check is conducted based on FEMA 356 [29] Table C1-3 Structural Performance Levels and Damage, which governed the allowable drift to be 0.7% for the Immediate Occupancy (IO) level, 2.5% for the Life Safety (LS) level, and 5% for the Collapse Prevention (CP) level. These interstory drift limits are specifically the performance level acceptance criteria of the steel moment frame at the structural level.

The comparison of the uncontrolled and controlled responses at the rooftop (20th story) demonstrates the effectiveness of the active control system. The control system could reduce the peak and the Root Mean Square (RMS) displacement, velocity, and acceleration responses.

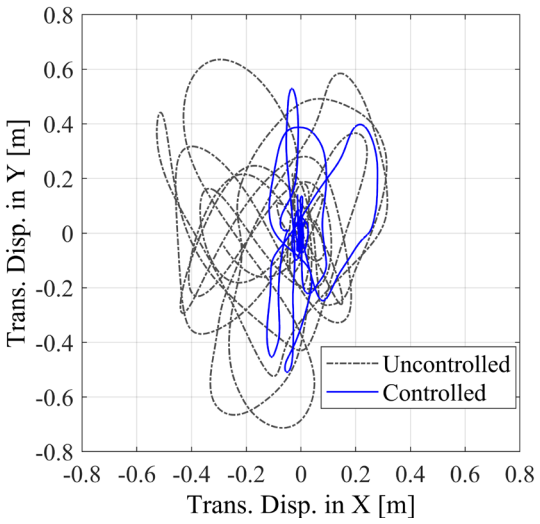

Fig. 2 Floor lateral displacement at the rooftop – Chi-Chi ground motion

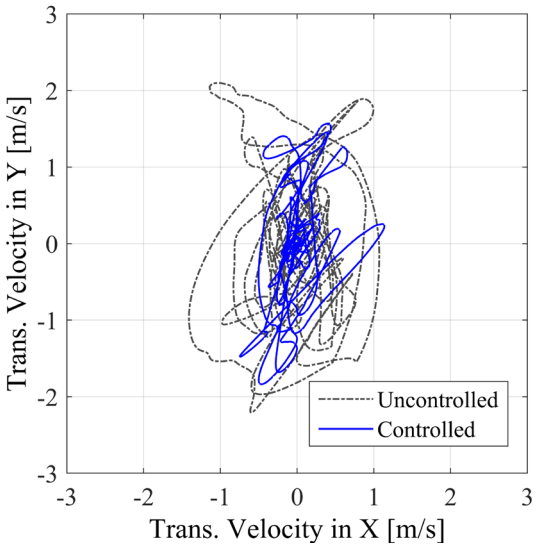

Fig. 3 Floor lateral absolute velocity at the rooftop – Chi-Chi ground motion

Figs. 2-4 show the rooftop's lateral displacement, velocity, and acceleration at the center of the mass. The control system could reduce the lateral displacement in the X- and Y-directions and the number of cyclic movements. The floor velocity and acceleration could be suppressed significantly, which is beneficial for serviceability and operational performance. The reduction of displacement also contributes to the structure's interstory drift reduction, which may lead to lesser damage.

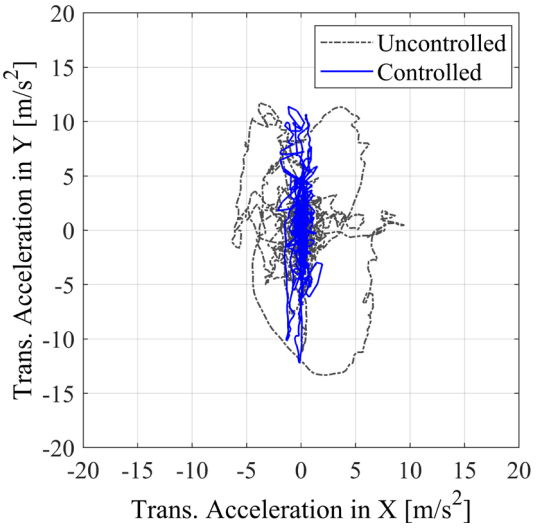

Fig. 4 Floor lateral absolute acceleration at rooftop – Chi-Chi ground motion

Based on FEMA 356, the control system could alleviate the performance level to be below the IO level except for the Chi-Chi 1999 record, which was initially beyond the CP level and is now experiencing the IO-to-LS level. Nevertheless, the control system may prevent the building from collapsing for that corresponding Chi-Chi record. As for the rest of the records, the performance level could be increased from LS-to-CP and IO-to-LS level to below IO level for both X- and Y-directions, as shown in Table 6-7.

Table 6. Performance level assessment at the structural level in X-direction

Ground Motion	Uncontrolled		Controlled	
	δ_{max}	Level	δ_{max}	Level
Imperial Valley	2.08%	IO to LS	0.66%	<IO
Kobe	2.07%	IO to LS	0.68%	<IO
Landers	3.80%	LS to CP	0.69%	<IO
Chi-Chi	5.03%	>CP	1.92%	IO to LS
Kocaeli	5.30%	>CP	0.67%	<IO

Table 7. Performance level assessment at the structural level in Y-direction

Ground Motion	Uncontrolled		Controlled	
	δ_{max}	Level	δ_{max}	Level
Imperial Valley	0.86%	IO to LS	0.63%	<IO
Kobe	0.85%	IO to LS	0.68%	<IO
Landers	0.76%	IO to LS	0.18%	<IO
Chi-Chi	1.23%	IO to LS	0.89%	IO to LS
Kocaeli	0.40%	<IO	0.40%	<IO

The structural response demonstration in terms of max interstory drift is demonstrated in Figs. 5-8. The max interstory drift could be reduced to around 61.8% to 87.3% of the uncontrolled case value. Despite the arbitrary optimal placement of the actuator devices, overall, the drift of each story could be reduced consistently.

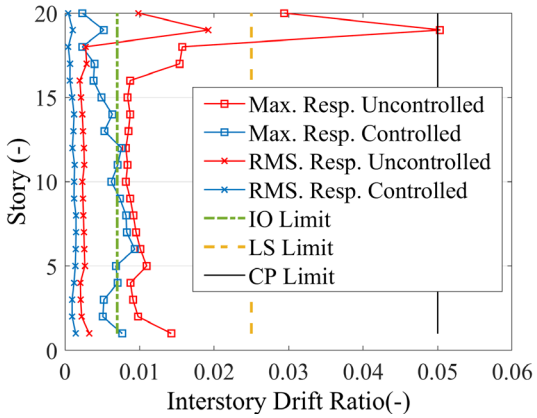

Fig. 5 Interstory drift in X-direction – Chi-Chi ground motion

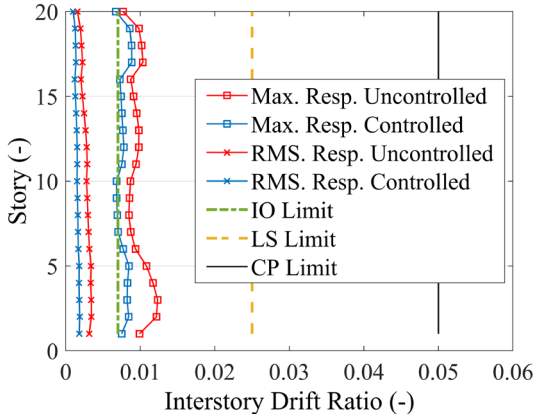

Fig. 6 Interstory drift in Y-direction – Chi-Chi ground motion

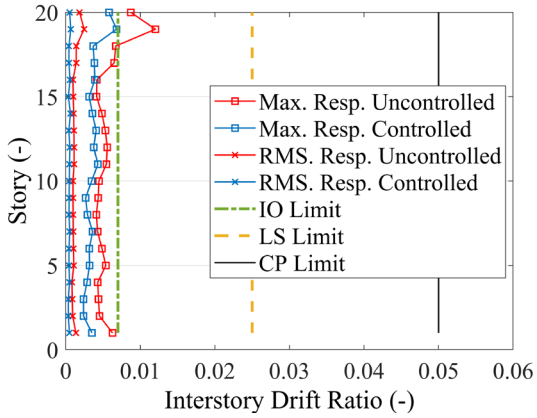

Fig. 7 Interstory drift in X-direction – Imperial Valley ground motion

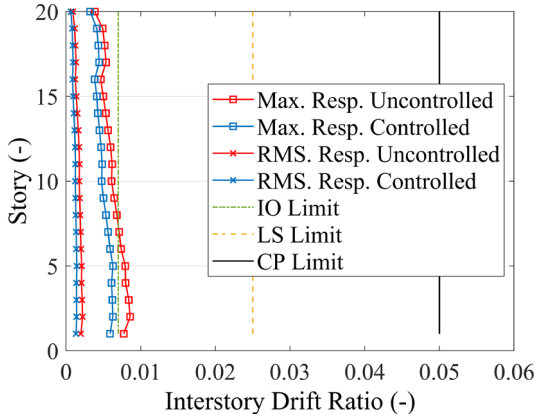

Fig. 8 Interstory drift in Y-direction – Imperial Valley ground motion

Fig. 9 demonstrates the performance improvement in the time domain. The DOF observed is located at the rooftop (20th story) where DOF 5429 to 5431 are X-, Y-, and Z-translational DOFs.

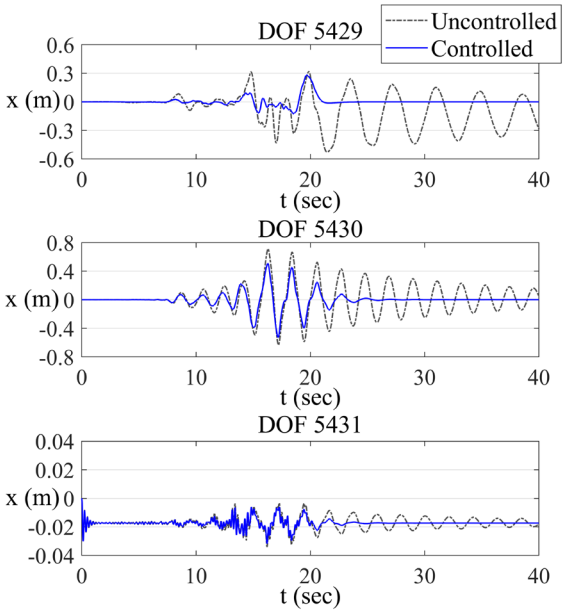

Fig. 9 Translational response in the time domain – Chi-Chi ground motion

The controlled response in Fig. 9 shows a significant reduction of permanent deformation in the X-direction, which is apparent after 20 seconds. The control system could dampen the cyclic movement significantly in both lateral and vertical directions. The amplitude location of each cycle between uncontrolled and controlled cases is similar, meaning a subtle structural stiffness change. The additional damping from the control system is apparent, where the amplitude of lateral displacement at the free vibration stage could be effectively damped out quickly.

4.2 Performance Level at the Element Level

The performance level check at the element level is conducted based on the ACE41-17 [30] Table 9-7.1 Modeling Parameters and Acceptance Criteria for Nonlinear Procedures – Structural Steel Beams and Columns – Flexural Action, which regulates the plastic rotation angle limit for the IO, LS, and CP level.

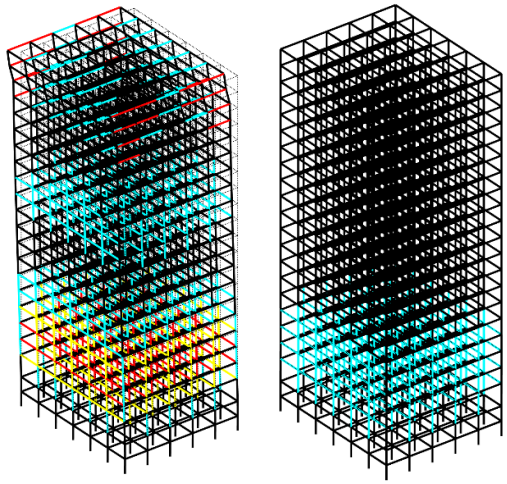

a. Uncontrolled b. Controlled

Fig. 10 Performance level check at elements level – Chi-Chi ground motion

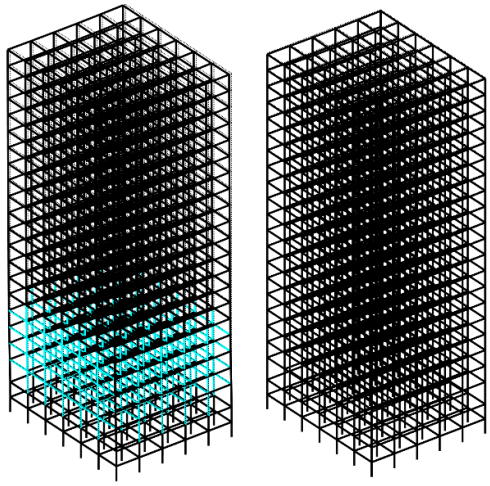

a. Uncontrolled b. Controlled

Fig.11 Performance level check at elements level – Imperial Valley ground motion

The visualization of the post-event condition of the building is depicted in Figs. 10-11. The color-coded elements explain the state they are experiencing at the final stage. The figures also visualize the permanent deformation of the building with a plot scale factor of 10. The non-linearity checks are conducted at two integration points for each element. The non-linearity could be checked without incorporating nonlinear spring elements that might capture the concentrated non-linearity.

Figs. 10-11 plotting legends: black (<IO), cyan (IO to LS), yellow (LS to CP), and red (>CP). The deformed shape is plotted based on the final state of the structure by the end of the observation duration. Zero padding is conducted to observe the free vibration response at the end of the duration. The active control system could prevent large permanent deformation for the Chi-Chi ground motion case, as shown in Fig. 10.

The elements are categorized based on the performance level to calculate the percentage distribution of each level, as presented in Table 8. The result could provide detailed information regarding critical elements that need to be retrofitted, thus making decision-making more accurate and economically efficient.

Table 8. Performance level assessment at the elements level

Ground Motion	Performance Level	Uncontrolled	Controlled
Imperial Valley	<IO	86.56%	100.00%
	IO to LS	13.44%	0.00%
	LS to CP	0.00%	0.00%
	>CP	0.00%	0.00%
Kobe	<IO	99.72%	100.00%
	IO to LS	0.28%	0.00%
	LS to CP	0.00%	0.00%
	>CP	0.00%	0.00%
Landers	<IO	99.84%	100.00%
	IO to LS	0.16%	0.00%
	LS to CP	0.00%	0.00%
	>CP	0.00%	0.00%
Chi-Chi	<IO	67.26%	86.56%
	IO to LS	18.99%	13.44%
	LS to CP	7.48%	0.00%
	>CP	6.28%	0.00%
Kocaeli	<IO	100.00%	100.00%
	IO to LS	0.00%	0.00%
	LS to CP	0.00%	0.00%
	>CP	0.00%	0.00%

Table (8) highlights the control system's efficacy in alleviating the building's performance level. Full Immediate Occupancy (IO) level is ensured for all the ground motions except for the Chi-Chi earthquake, where the controlled case could prevent the element from experiencing LS-to-CP and beyond CP level. Only 13.44% of the elements have the IO-to-LS level for the controlled case of the Chi-Chi ground motion, while the rest 86.56% are below the IO level.

4.3 Control Forces Demand

The control force demand indicates saturation due to actuator capacity limitation. The control force is limited to 1500 kN per device based on the information of the available actuator devices in the market. As for the Chi-Chi ground motion, the total control force per story is capped at 6000 kN since four devices are placed per floor. The control force demands of the Chi-Chi ground motion in the X- and Y-direction are shown in Figs. 12-13.

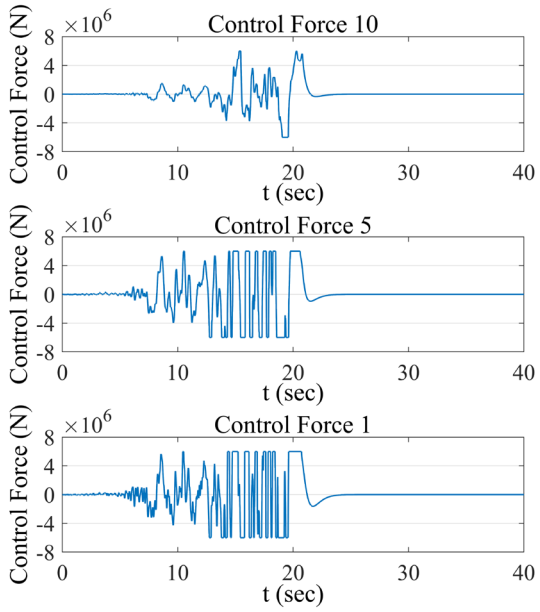

Fig. 12 Control force demand in X-Direction – Chi-Chi ground motion

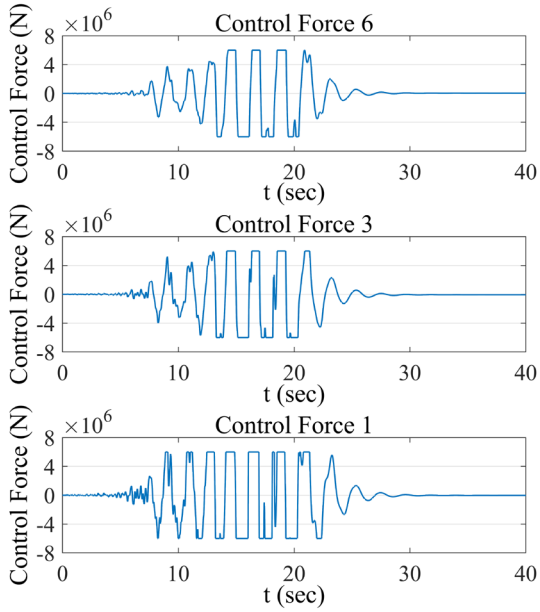

Fig. 13 Control force demand in X-Direction – Chi-Chi ground motion

The control force saturation is experienced in most of the controlled stories and is caused by the large control demand of the Chi-Chi record. The control force demands at the lower stories are generally larger than the upper stories of the building. After approximately 25 seconds, the control force demand goes to zero as the structure has been brought to its stationary condition.

4.4 Frequency Response Function

The frequency response functions are demonstrated using the Chi-Chi actuator configuration. The dynamic amplification factor could be significantly reduced for the first few dominant modes where the peak amplification is no longer apparent for the controlled case in the X-direction. The system is also experiencing phase changes, which is evident in the X-direction.

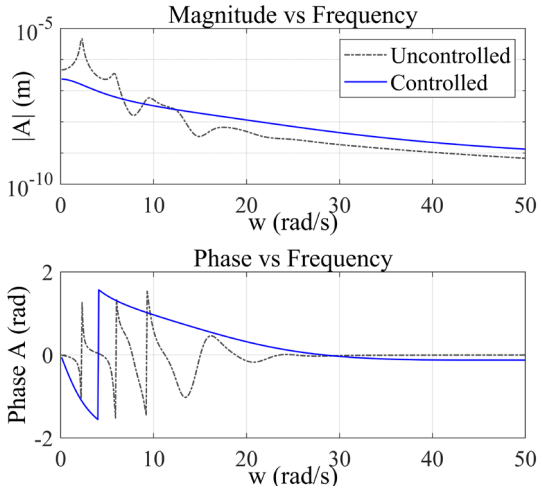

Fig. 14 Frequency response function on X-Direction – Chi-Chi ground motion

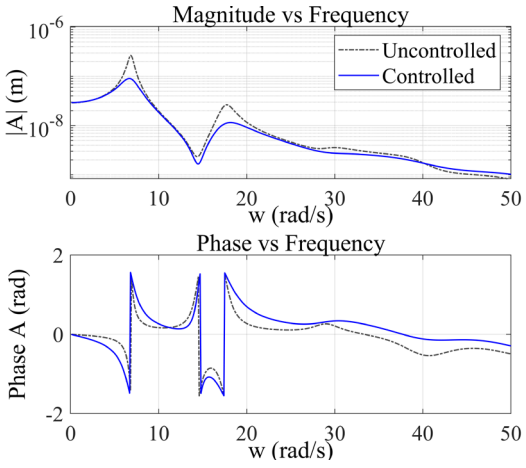

Fig. 15 Frequency response function on Y-Direction – Chi-Chi ground motion

On the other hand, the dynamic amplification factor of the Y-direction experiences a slight reduction because the control force demand in the Y-direction is lesser than in the X-direction. The uncontrolled interstory drift in the Y-direction only exceeds a small margin from the 0.7% limit.

5. CONCLUSION

The optimized control system is beneficial in minimizing and preventing plastic rotation angle and also improving the performance level of the building while ensuring an economical solution. The control system could effectively reduce the max interstory drift in both excitation directions, where the interstory drifts are reduced from a range of 2.07%-5.30% to 0.66%-1.92% in the X-direction and from a range of 0.4%-1.23% to 0.4%-0.89% in the Y-direction.

The control system could realize the Immediate Occupancy (IO) level for most seismic records, which initially ranged from Life Safety (LS) to beyond Collapse Prevention (>CP) level. The performance levels of the structural elements are improved for all ground motion to be 100% below the IO level except for the Chi-Chi record, where only 13.44% of elements are experiencing the IO-to-LS level, while the rest 86.56% of elements are below the IO level.

The nonlinear time history analysis results have proven the active control system's efficacy in improving the building's performance levels at the structural and element levels, as demonstrated in the time and frequency domain analyses. The performance level assessment could provide detailed information regarding critical elements, thus making decision-making more accurate and efficient.

6. ACKNOWLEDGMENTS

This research was supported and funded by Institut Teknologi Bandung through the Program of Research, Community Service and Innovation (P2MI) – Faculty of Civil and Environmental Engineering (FTSL).

7. REFERENCES

[1] Singh, A., and Palissery, S., "Preferred Seismic Performance Attainment in Important Buildings," Engineering Failure Analysis, vol. 158, 2024, pp. 1-19, doi: 10.1016/j.engfailanal.2023.107952.

[2] Harris, J., and Speicher, M., "Assessment of performance-based seismic design methods in ASCE 41 for new steel buildings: Special moment frames," Earthquake Spectra, vol. 34, no. 3, 2018, pp. 977–999, doi: 10.1193/050117EQS079EP.

[3] Castillo, J. G. S., Bruneau, M., and Elhami-Khorasani, N., "Seismic resilience of building inventory towards resilient cities," Resilient Cities and Structures, vol. 1, no. 1, 2022, pp. 1–12, doi: 10.1016/j.rcns.2022.03.002.

[4] Christopoulos, C., and Zhong, C., "Towards understanding, estimating and mitigating higher-mode effects for more resilient tall buildings," Resilient Cities and Structures, vol. 1, no. 1, 2022, pp. 53–64, doi: 10.1016/j.rcns.2022.03.005.

[5] Jiwapatria, S., Setio, H. D., Sidi, I. D., and Kusumaningrum, P., "Multi-objective optimization of active control system using population guidance and modified reference-point-based NSGA-II," Results in Control and Optimization, vol. 16, 2024, pp. 1-17, doi: 10.1016/j.rico.2024.100453.

[6] Kazemi, F., Asgarkhani, N., and Jankowski, R., "Enhancing seismic performance of steel buildings having semi-rigid connection with infill masonry walls considering soil type effects," Soil Dynamics and Earthquake Engineering, vol. 177, 2024, pp. 1-23, doi: 10.1016/j.soildyn.2023.108396.

[7] Malik, U. J., Najam, F. A., Khokhar, S. A., Rehman, F., and Riaz, R. D., "Advancing seismic resilience: Performance-based assessment of mid-rise and high-rise engineered cementitious composite (ECC) Buildings," Case Studies in Construction Materials, vol. 20, 2024, pp. 1-20, doi: 10.1016/j.cscm.2023.e02732.

[8] Fauzan, Hakam, A. Ismail, F. A., Osman, J. V., and Al, J. Z., "Experimental Investigation of Hollow Brick Unreinforced Masonry Building Retrofitted by Ferrocement Layers," International Journal of GEOMATE, vol. 24, no. 102, 2023, pp. 117–124, doi: 10.21660/2023.102.s8622.

[9] Sunarno, Y., Tjaronge, M. W., Irmawaty, R. and Muhiddin, A. B. "Behaviour of RC Frame using Precast Foam Concrete Strengthened With CFRP as an Infill Wall under Horizontal Cyclic Loading," International Journal of GEOMATE, vol. 25, no. 110, 2023, pp. 98–105, doi: 10.21660/2023.110.3975.

[10] Orientilize, M., Prakoso, W. A., Lase, Y., Purnomo, S. and Sumartono, I. H. "Study of Repaired Spun Pile to Pile Cap Connections Containing Fractured Reinforcements using FRP," International Journal of GEOMATE, vol. 25, no. 110, pp. 114–122, 2023, doi: 10.21660/2023.110.3987.

[11] Setio, H. D., and Jiwapatria, S., "Smart Structure Technology for Resilient Building and Infrastructures Against Natural Hazards: Past Experiences, Opportunities, and Challenges,"

Proceedings of 6th International Conference on Civil Engineering and Architecture, Vol. 1, 2024, pp. 162–174. doi: 10.1007/978-981-97-5311-6_16.

[12] Martelli, A., Forni, M., and Panza, G., "Features, recent application and conditions for the correct use of seismic isolation systems," Transactions on State of the Art in Science and Engineering, vol. 59, 2012, pp. 1-15, doi: 10.2495/978-1-84564-/6.

[13] Chang, K., Hwang, J., Sung, Y., Wang, S., Yu, C., Lin, W., and Yang, C., "Recent Progress and Experience in Taiwan on Passive Control Technology," 16th World Conference on Seismic Isolation, Energy Dissipation and Active Vibration Control of Structures, 2019, pp. 718-729, doi:10.37153/2686-7974-2019-16-718-729.

[14] Nochebuena-Mora, E., Mendes, N., Lourenço, P. B., and Covas, J. A., "Vibration control systems: A review of their application to historical unreinforced masonry buildings," Journal of Building Engineering, vol. 44, 2021, pp. 1-15, doi: 10.1016/j.jobe.2021.103333.

[15] Javanmardi, A., Ghaedi, K., Huang, F., Hanif, M. U., and Tabrizikahou, A., "Application of Structural Control Systems for the Cables of Cable-Stayed Bridges: State-of-the-Art and State-of-the-Practice," Archives of Computational Methods in Engineering, vol. 29, no. 3, 2022, pp. 1611–1641, doi: 10.1007/s11831-021-09632-4.

[16] Almajhali, K. Y. M., "Review on passive energy dissipation devices and techniques of installation for high rise building structures," Structures, vol. 51, 2023, pp. 1019-1029, doi: 10.1016/j.istruc.2023.03.025.

[17] Mansour, M. H., Hussein, M. M., and Akl, A. Y., "Assessment Of Base-Isolated Buildings Designed using International Damping Modification Factors," International Journal of GEOMATE, vol. 21, no. 83, 2021, pp. 1–10, doi: 10.21660/2021.83.j2121.

[18] Amin, N. M., Ayub, N., and Alisibramulisi, A., "Design of base isolated reinforced concrete building subjected to seismic excitation using EC 8," International Journal of GEOMATE, vol. 17, no. 63, 2019, pp. 23–28, doi: 10.21660/2019.63.4672.

[19] Li, J. and Wang, W., "Seismic design of low-rise steel building frames with self-centering hybrid damping connections," Resilient Cities and Structures, vol. 1, no. 2, 2022, pp. 10–22, doi: 10.1016/j.rcns.2022.06.002.

[20] Chen, K., Tsampras, G., and Lee, K., "Structural connection with predetermined discrete variable friction forces," Resilient Cities and Structures, vol. 2, no. 1, 2023, pp. 1–17, doi: 10.1016/j.rcns.2023.02.006.

[21] Dadkhah, M., Kamgar, R., Heidarzadeh, H., Jakubczyk-Galczyńska, A., and Jankowski, R., "Improvement of performance level of steel moment-resisting frames using tuned mass damper system," Applied Sciences, vol. 10, no. 10, 2020, pp. 1-27, doi: 10.3390/APP10103403.

[22] Ji, X., Jia, R., Wang, L., Wang, M., and Wu, X., "Seismic design and performance assessment of a retrofitted building with tuned viscous mass dampers (TVMD)," Eng. Struct., vol. 305, 2024, pp. 1-16, doi: 10.1016/j.engstruct.2024.117688.

[23] Gómez, F., and Yu, W., "Discrete-time tri-directional active control of building structures," Eng. Struct., vol. 243, 2021, pp. 1-11, doi: 10.1016/j.engstruct.2021.112689.

[24] Takagi, J., and Wada, A., "Recent earthquakes and the need for a new philosophy for earthquake-resistant design," Soil Dynamics and Earthquake Engineering, vol. 119, 2019, pp. 499–507, doi: 10.1016/j.soildyn.2017.11.024.

[25] Saini, D., Dokhaei, B., Shafei, B., and Alipour, A., "Performance evaluation of high-rise buildings using database-assisted design approach," Structural Safety, vol. 109, 2024, pp. 1-19, doi: 10.1016/j.strusafe.2024.102447.

[26] Athanasiou, A., Tirca, L., and Stathopoulos, T., "Performance-based wind and earthquake design framework for tall steel buildings with ductile detailing," Journal of Wind Engineering and Industrial Aerodynamics, vol. 240, 2023, pp. 1-13, doi: 10.1016/j.jweia.2023.105492.

[27] Ijmulwar, S. S., and Patro, S. K., "Seismic design of reinforced concrete buildings equipped with viscous dampers using simplified performance-based approach," Structures, vol. 61, 2024, pp. 1-16, doi: 10.1016/j.istruc.2024.106020.

[28] Ohtori, Y., Christenson, R. E., Spencer, B. F., and Dyke, S. J., "Benchmark Control Problems for Seismically Excited Nonlinear Buildings," J Eng Mech, vol. 130, no. 4, 2004, pp. 366–385, doi: 10.1061/(asce)0733-9399(2004)130:4(366).

[29] FEMA, "FEMA 356 - Prestandard and Commentary For The Seismic Rehabilitation Of Buildings", 2000.

[30] ASCE/SEI, ASCE 41-17: Seismic Evaluation and Retrofit of Existing Buildings, 2017.

[31] Deb, K., Pratap, A., Agarwal, S., and Meyarivan, T., "A fast and elitist multiobjective genetic algorithm: NSGA-II," IEEE Transactions on Evolutionary Computation, vol. 6, no. 2, 2002, pp. 182–197, doi: 10.1109/4235.996017.